DESIGN OF ROBUST CONTROLLER FOR STATCOM APPLIED TO LARGE INDUCTION MOTOR USING GRAPHICAL LOOP SHAPING METHOD

Mahdi Hedayati [1] **Norman Mariun** [1] **Mojgan Hojabri** [2]

1 Department of Electrical & Electronics Engineering, Faculty of Engineering, University Putra Malaysia, 43400 UPM, Serdang, Selangor, Malaysia,

2 Faculty of Electrical and Electronics Engineering, University Malaysia Pahang (UMP), 26600 Pekan, Pahang, Malaysia

Abstract: *Between the different robust H-Infinity methods to design the controller for FACTS, loop shaping is known to be one of the effective and feasible methods. This research presents an investigation on H-Infinity loop shaping procedure via Graphical Loop Shaping (GLS) for STATCOM installed at terminals of a large induction motor. The dynamic behavior of induction motor is analyzed while the uncertainty of system parameters and STATCOM parameters are considered and will be compared with conventional PI controller.*
Simulation results prove that GLS method has better dynamic response and more robust than PI controller against variation of system parameters and STATCOM Parameters, so in a specified operating point, even the system goes to instability.

Keywords: STATCOM; Robust Control; Graphical Loop Shaping, Uncertainty Modeling

1. Introduction

Conventional PI (or PID controller) is one of the best known as industrial process controller and despite a many research and the great number of different solutions proposed, most industrial control systems are based on this conventional regulator. In this method, the system linearized around nominal point. Although PI controller has some disadvantages such as: the high starting overshoot, long adjusting time, sensitivity to controller gains and lethargic response due to sudden disturbance [1, 2], the mentioned controller has adequate response at this point. Shunt FACTS devices like SVC or STATCOM are employed in industrial applications of Induction motors to correct disturbance during the starting that is ordinary in form of voltage sag [3, 4] . These types of compensators raise the motor speeding up and enhance the voltage profile [5-7].But FACTS devices and the other power system elements have nonlinearity nature and acquiring a precise nonlinear model that exactly is compatible with the plant at all working points is a difficult to attain. So, most of advanced controllers are generally designed utilizing a linear model of the process based on fixed information of the plant that is incomplete and defective; consequently, control quality may decline when working circumstances vary [8].
Besides, there exists the uncertainty in the system that makes it hard to design a satisfied controller for the FACTS that assures fast and stable regulation under all operating conditions. The main source of trouble is that the P_{nom} (open loop plant) may be incorrect or may vary with time. In particular, incorrectness in P_{nom} may create problems because the plant is part of the feedback loop. To engage in a problem, instead of using a single model, a model with $P = P_{nom} + E$ should be considered, where E is the uncertainty or perturbation [9].
In view of these problems, robust control design methods is appeared to be convenient, since they present linear controllers with acceptable stability margins [10]. The principle of robust control is to model the uncertainties themselves and to include them in the design method of the control system with the target of covering stability and performance criteria at all working points[11, 12]. The change of operating conditions is considered as a source of unstructured uncertainty in the linearized system model. Another important matter is the ability of controller to remove the effects of external disturbances on system execution [13].
Among all the presented robust H_∞ techniques to design the controller of shunt FACTS, the H_∞ loop shaping procedure has been chosen, because this method have some benefits when compared with other H_∞ design techniques [14-17]. The main advantage of H_∞ loop shaping method is that it does not require the so called γ – iteration to obtain the optimal controller. Also, there are obtainable comparatively simple formulas to propose the controller and it is proportionately easy to perform based on classical loop shaping ideas [8, 9]. Graphical Loop Shaping (GLS) method is investigated to propose H_∞ loop shaping theory.
The rest of this paper is organized as follows. First, the GLS method is presented. Next, the design of the

controller utilizing this procedure for STATCOM connected to a large induction motor is specified and simulation result for step response of motor's rotor speed based on this method is shown and the suggested controller will be compared with a conventional PI controller. Finally the uncertainties of system parameters are considered on behavior of proposed controllers.

2. Graphical Loop Shaping (GLS) Method

Loop shaping is a graphical method to design suitable controller fulfilling robust stability and performance [18]. In this section, a concise theory of the uncertainty modeling, robust stability and robust performance criteria will be presented to acquire a robust control design algorithm.

2.1. Uncertainty Modeling

Assume that the linearized plant having a nominal transfer function P consists a set of transfer functions $\boldsymbol{P}$. Consider that the perturbed transfer function, consequence from the variations in operating circumstances, may be stated as:

$$\tilde{P} = (1 + \Omega W_2)P \qquad (1)$$

Hence, W_2 is a fixed stable transfer function that has been defined before as uncertainty weight, also called the weighting function and Ω is a variable transfer function satisfying $\|\Omega\|_\infty < 1$.

Definition: $\| \Delta_P \|_\infty = sup_\omega |\Delta_P (j\omega)|$ is the infinity norm of a function Δ_P and is the largest value of gain on a bode magnitude plot. For asymptotically stable transfer function, the special form of the infinity norm, called H infinity norm (H_∞ norm) is applied [10, 19].

The linearized state model for small perturbation around a nominal operating circumstance is expressed for time invarrying system as:

$$X^0 = AX + BU \qquad (2)$$

$$Y = CX + DU \qquad (3)$$

Taking the Laplace transform of Equations 2 and 3, we get:

$$sX(s) = AX(s) + BU(s) \qquad (4)$$

$$Y(s) = CX(s) = C(sI - A)^{-1}BU(s) + DU(s) \qquad (5)$$

Therefore, the plant transfer function will be calculated as:

$$P = \frac{Y(s)}{U(s)} = C(sI - A)^{-1}B + D \qquad (6)$$

With considering $\|\Omega\|_\infty < 1$, the multiplicative uncertainty model (Equation 1) is rewritten as:

$$\left|\frac{\tilde{P}(j\omega)}{P(j\omega)} - 1\right| \leq W_2(j\omega) \qquad \forall\ \omega \qquad (7)$$

So, $W_2(j\omega)$ gives the uncertainty profile, and in the frequency plane is the upper boundary of all the normalized plant transfer functions away from 1 [20, 21].

2.2 Robust Stability and Robust Performance criteria

Considering a feedback system with reference trajectory r and plant output y as specified in Figure1. The tracking error signal is defined as $e = r - y$, thus forming the negative feedback loop. The sensitivity function is written as

$$S = \frac{e}{r} = \frac{1}{1 + PC} \qquad (8)$$

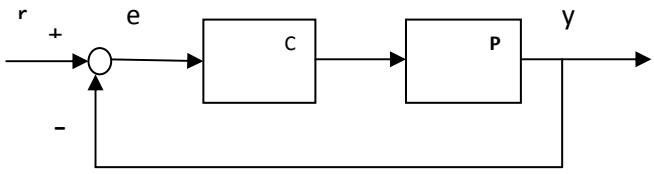

Figure 1: Unity feedback with controller

Where P symbolize the plant transfer function, and C is the controller. The controller will provide stability if it gives internal stability for every plant in the uncertainty set $\boldsymbol{P}$. If L represents the open loop transfer function $L = PC$, then the sensitivity transfer function will be written as:

$$S = \frac{1}{1 + L} \qquad (9)$$

The complimentary transfer function or the output-input transfer function is:

$$\text{T=1-}S = \frac{PC}{1+PC} = \frac{L}{1+L} \qquad (10)$$

Performance requirements of a feedback controller, utilizing the nominal plant model can be shaped in terms of the Nyquist plot. The reqirement for adequate performance with plant uncertainty is a combination of the two requirements. The fist one is a condition for nominal performance in the presence of multiplicative uncertainty parameterized with $W_1(j\omega)$ that expressed as:

$$|W_1(j\omega)S(j\omega)| < 1 \qquad \forall\omega \qquad (11)$$

The second one is necessary and sufficient condition for robust stability in the presence of multiplicative uncertainty parameterized with $W_2(j\omega)$ that determined as follows:

$$|W_2(j\omega)T(j\omega)| < 1 \qquad \forall\omega \qquad (12)$$

The requirement for adequate performance with plant uncertainty is a combination of the above two requirements. Hence it is clear that with multiplicative uncertainty, nominal performance plus robust stability almost guarantee robust performance [10]. Graphically, as shown in the Figure 2, the disk at the critical point with radius $|W_1(j\omega)|$, should not intersect the disk of radius $|W_2(j\omega)P(j\omega)C(j\omega)|$, centered on the nominal locus $P(j\omega)C(j\omega)$ [22]. This can be written as:

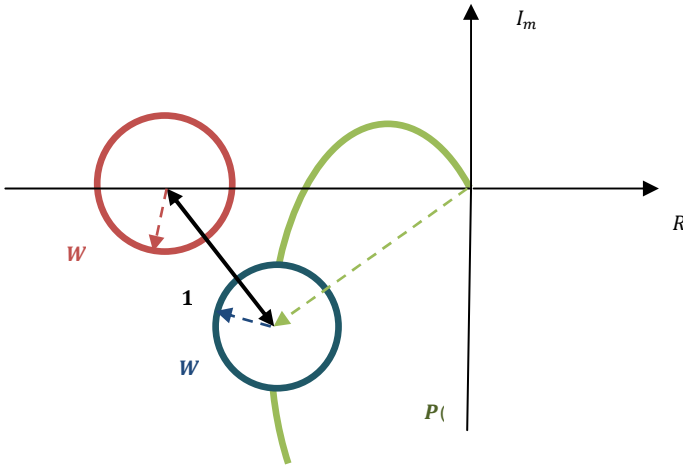

Figure 2: Nyquist plane construction for robust performance under multiplicative uncertainty

$$|W_1(j\omega)| + |W_2(j\omega)\,P(j\omega)C(j\omega)| < |1 + P(j\omega)C(j\omega)| \;\forall\omega \qquad (13)$$

Dividing by $|1 + P(j\omega)C(j\omega)|$ gives:

$$\frac{|W_1(j\omega)|}{|1 + P(j\omega)C(j\omega)|} + \frac{|W_2(j\omega)\,P(j\omega)C(j\omega)|}{|1 + P(j\omega)C(j\omega)|} < 1 \quad \forall\omega \qquad (14)$$

Or

$$|W_1(j\omega)S(j\omega)| + |W_2(j\omega)T(j\omega)| < 1 \qquad \forall\omega \qquad (15)$$

The Equation 15 is necessary and sufficient condition for robust stability and performance in the presence of multiplicative uncertainty.

2.3 GLS Technique

Loop shaping is a graphical method to design a suitable controller C fulfilling robust stability and performance criterion specified in sect 2.2. The basic idea of this method is explained and applied in [20-22] to obtain an approximate solution of this problem, which can be readily extended to different weighting transfer functions. The first step is to construct the loop transfer function L to satisfy the robust performance criterion and then to acquire the controller from the relationship $C = \frac{L}{P}$. Internal stability of the plants and properness of C represent the constraints of the method. Condition on L is such that PC should not have any pole –zero cancellation. An essential condition for robustness is that either or both $W_1(j\omega)$ and $W_2(j\omega)$ must be less than 1 at any frequency. The robustness condition given in Equation 15 can be obtained as the following equation:

$$\left|W_1(j\omega)(1 + L(j\omega))^{-1}\right| + \left|W_2(j\omega)L(j\omega)(1 + L(j\omega))^{-1}\right| < 1 \quad \forall\omega \qquad (16)$$

At low frequency, $S(j\omega)$ is small (S→0 and T→1), because $L(j\omega)$ is large, therefore $|W_2(j\omega)T(j\omega)|$ <1 will conclude that $W_2(j\omega)$ <1. At high frequency, $T(j\omega)$ is small (S→1 and T→0), because $L(j\omega)$ is small, therefore $|W_1(j\omega)S(j\omega)|$ <1 will conclude that $W_1(j\omega)$ <1. Sufficient conditions to fulfill the robust performance condition in these regions are [8, 20, 22]:

$$\text{At low frequency} : |L| > \frac{|W_1|+1}{1-|W_2|} \quad \text{or} \quad |L| > \frac{|W_1|}{1-|W_2|} \qquad (17)$$

$$\text{At high frequency} : |L| < \frac{1-|W_1|}{1+|W_2|} \quad \text{or} \quad |L| < \frac{1-|W_1|}{|W_2|} \text{ or } |L| < \frac{1}{|W_2|} \qquad (18)$$

2.4 The Algorithm of GLS Procedure Based on H_∞ Theory

The algorithm to produce a control transfer function C based on GLS method so that robust stability and robust performance requirements are satisfied, specified by the flowchart of Figure 3.

3. System Modeling

The system under study is the machine, a network and infinite bus where STATCOM is installed on the terminal of the induction motor. Figure 3 shows the system modeling with a STATCOM which consists of DC capacitor, a three phase GTO based VSC and a step down transformer.

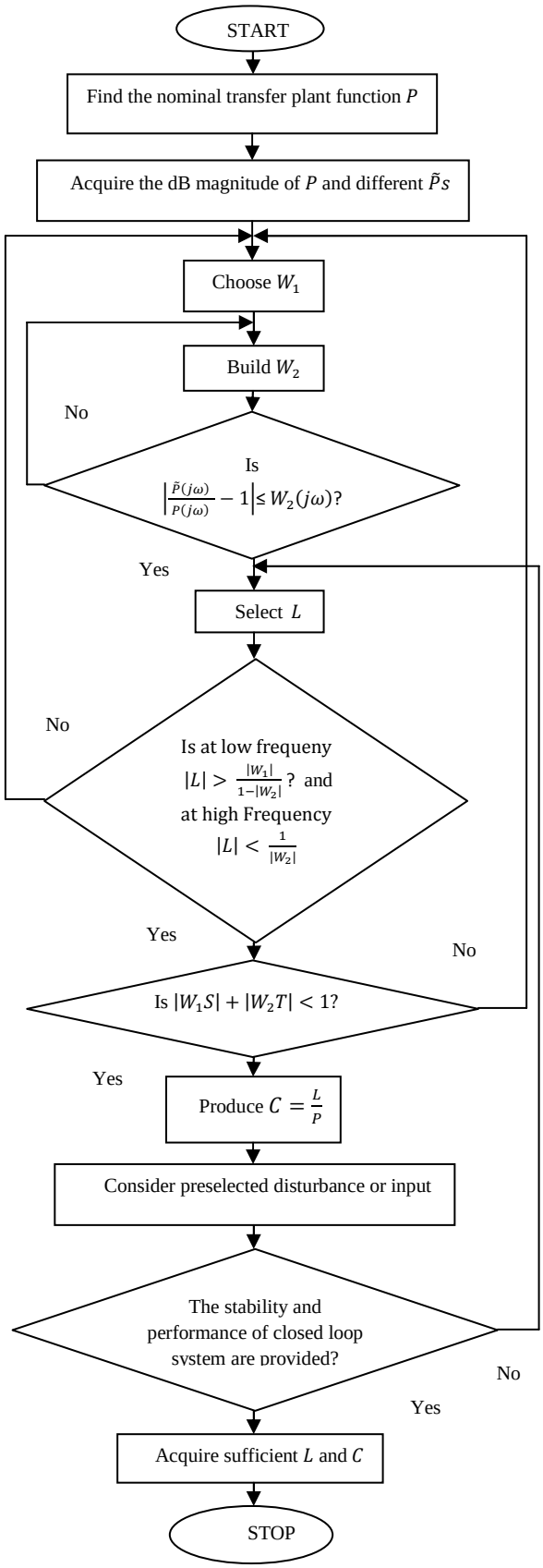

Figure 3: Algorithm flowchart of H_∞ GLS method

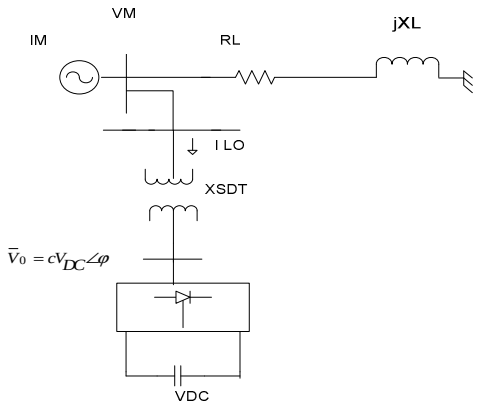

Figure 4: System modeling with a STATCOM

4. Linearized Model of System with STATCOM

For the construction of electromechanical mode damping controllers, the linearized supplementary model around a nominal operation point is commonly utilized. By linearizing the system equations at a given operating state that specified as follows:

$\boldsymbol{V_{Line}\,(rated)}$**=2300 V,** $\boldsymbol{Power\ (rated)}$ **= 2250 hp,** $\boldsymbol{f}$**=60 Hz,** $\boldsymbol{X_{ls}}$**=0.0716,** $\boldsymbol{X'_{lr}}$**=0.0716,** $\boldsymbol{X_M}$**=4.13,** $\boldsymbol{X_{ss}}$**=4.2,** $\boldsymbol{X'_{rr}}$**=4.2, D=0.6,** $\boldsymbol{R_{sm}}$**=0.0091,** $\boldsymbol{R'_{rm}}$**=0.697,** $\boldsymbol{\varphi_{qsm0}}$**=0.0023,** $\boldsymbol{\varphi_{dsm0}}$**=1.0364,** $\boldsymbol{\varphi'_{qrm0}}$**=0.0026,** $\boldsymbol{\varphi'_{drm0}}$**=1.0187,** $\boldsymbol{\omega_b}$**=377 rad/s,** $\frac{\boldsymbol{\omega_{rm0}}}{\boldsymbol{\omega_b}}$ **=1,** $\boldsymbol{P_m}$**=4,** $\boldsymbol{J_m}$**=63.87**$\boldsymbol{Kgr.m^2}$**,** $\boldsymbol{X_L}$**=0.04,** $\boldsymbol{R_L}$**=0,** $\boldsymbol{V_{q\infty}}$**=1,** $\boldsymbol{V_{d\infty}}$**=0,** $\boldsymbol{X_{SDT}}$**= 0.015,** $\boldsymbol{C_0}$**=1,** $\boldsymbol{\varphi_0}$**=1 rad,** $\boldsymbol{V_{DC0}}$**=1,** $\boldsymbol{C_{DC}}$**=1,** $\boldsymbol{I_{Lod0}}$**=2.70,** $\boldsymbol{I_{Loq0}}$**=9.82,** $\boldsymbol{V_{qsmo_{STATCOM}}}$**=0.88,** $\boldsymbol{V_{dsm0_{STATCOM}}}$**=0.3** $\boldsymbol{V_{to_{STATCOM}}}$**=0.97,**

the linearized model for the system with STATCOM can be obtained. The lineraized model for system with a STATCOM can be written as:

$$\begin{bmatrix} \Delta\psi_{qsm} \\ \Delta\psi_{dsm} \\ \Delta\psi'_{qrm} \\ \Delta\psi'_{drm} \\ \frac{\Delta\omega_{rm}}{\omega_b} \\ \Delta V_{DC} \end{bmatrix}^0 = [A_{STATCOM}]_{6*6} \begin{bmatrix} \Delta\psi_{qsm} \\ \Delta\psi_{dsm} \\ \Delta\psi'_{qrm} \\ \Delta\psi'_{drm} \\ \frac{\Delta\omega_{rm}}{\omega_b} \\ \Delta V_{DC} \end{bmatrix} + [B_{STATCOM}]_{6*2} \begin{bmatrix} \Delta C \\ \Delta\varphi \end{bmatrix} \quad (19)$$

$$\left[\frac{\Delta\omega_{rm}}{\omega_b}\right]^0 = \left[C_{STATCOM_\omega}\right]_{1*6} \begin{bmatrix} \Delta\psi_{qsm} \\ \Delta\psi_{dsm} \\ \Delta\psi'_{qrm} \\ \Delta\psi'_{drm} \\ \frac{\Delta\omega_{rm}}{\omega_b} \\ \Delta V_{DC} \end{bmatrix} \quad (20)$$

Matrices $[A_{STATCOM}]$, $[B_{STATCOM}]$ and $\left[C_{STATCOM_\omega}\right]$ are identified as follows:

$$[A_{STATCOM}] = \omega_b \begin{bmatrix} A_{11} & A_{12} & A_{13} & A_{14} & A_{15} & A_{16} \\ A_{21} & A_{22} & A_{23} & A_{24} & A_{25} & A_{26} \\ A_{31} & A_{32} & A_{33} & A_{34} & A_{35} & A_{36} \\ A_{41} & A_{42} & A_{43} & A_{44} & A_{45} & A_{46} \\ A_{51} & A_{52} & A_{53} & A_{54} & A_{55} & A_{56} \\ A_{61} & A_{62} & A_{63} & A_{64} & A_{65} & A_{66} \end{bmatrix} \quad (21)$$

$$[B_{STATCOM}] = \begin{bmatrix} B_{11} & B_{12} \\ B_{21} & B_{22} \\ B_{31} & B_{32} \\ B_{41} & B_{42} \\ B_{51} & B_{52} \\ B_{61} & B_{62} \end{bmatrix} \quad (22)$$

$$\left[C_{STATCOM_\omega}\right] = [0\ 0\ 0\ 0\ 0\ 1] \quad (23)$$

That

$$A_{11}=-\frac{R_{sm}}{D}\mathrm{X}'_{\mathrm{rr}}, A_{12}=-\left(1+\frac{X_L}{D}\frac{\mathrm{X}'_{\mathrm{rr}}}{FF_B}\right), A_{13}=\frac{R_{sm}}{D}X_M,\ A_{14}=\frac{X_L}{D}\frac{X_M}{FF_B}$$
$$A_{15}=0, A_{16}=\frac{X_L C_0 \sin\varphi_0}{X_{SDT}FF_B},\ A_{21}=-A_{12}\ ,\ A_{22}=A_{11}\ ,\ A_{23}=-A_{14}$$
$$A_{24}=A_{13}, A_{16}=\frac{X_L C_0 \cos\varphi_0}{X_{SDT}FF_B},\ A_{31}=\frac{R'_{rm}}{D}X_M, A_{32}=0, A_{33}=-\frac{R'_{rm}}{D}\mathrm{X}_{\mathrm{ss}}$$
$$A_{34}=\left(1-\frac{\omega_{rm0}}{\omega_b}\right), A_{35}=\psi'_{drm0}, A_{36}=0, A_{41}=0, A_{42}=A_{31} \quad (24)$$
$$A_{43}=-A_{34}\ , A_{44}=A_{33}, A_{45}=-\psi'_{qrm0}\ , A_{46}=0$$
$$A_{51}=\frac{1}{2H_M\omega_b}\frac{X_M}{D}\psi'_{drm0}, A_{52}=\frac{-1}{2H_M\omega_b}\frac{X_M}{D}\psi'_{qrm0}$$
$$A_{53}=\frac{-1}{2H_M\omega_b}\frac{X_M}{D}\psi_{dsm0}, A_{54}=\frac{1}{2H_M\omega_b}\frac{X_M}{D}\psi_{qsm0}$$
$$A_{55}=A_{56}=0, A_{61}=-GG_2\left(\frac{X_L}{D}\frac{\mathrm{X}'_{\mathrm{rr}}}{FF_B}\right), A_{62}=-GG_1\left(\frac{X_L}{D}\frac{\mathrm{X}'_{\mathrm{rr}}}{FF_B}\right)$$
$$A_{63}=GG_2\left(\frac{X_L}{D}\frac{X_M}{FF_B}\right), A_{62}=GG_1\left(\frac{X_L}{D}\frac{X_M}{FF_B}\right), A_{65}=A_{66}=0$$

$$B_{11}=\omega_b\frac{X_L V_{DC0}\sin\varphi_0}{X_{SDT}FF_B},$$
$$B_{12}=\omega_b\frac{X_L C_0 V_{DC0}\cos\varphi_0}{X_{SDT}FF_B}, B_{21}=\omega_b\frac{X_L V_{DC0}\cos\varphi_0}{X_{SDT}FF_B}$$
$$B_{22}=-\frac{X_L C_0 V_{DC0}\sin\varphi_0}{X_{SDT}FF_B}, B_{31}=B_{32}=B_{41}=0 \quad (25)$$
$$B_{42}=B_{51}=B_{52}=0$$
$$B_{61}=\frac{I_{Lod0}\cos\varphi_0+I_{Loq0}\sin\varphi_0}{C_{DC}}$$
$$B_{62}=\frac{-C_0\, I_{Lod0}\sin\varphi_0+C_0\, I_{Loq0}\cos\varphi_0}{C_{DC}}+\frac{{C_0}^2 V_{DC0}}{C_{DC}X_{SDT}}\left(\frac{X_L}{FF_B}-1\right)$$

And

$$GG_1=\frac{C_0\cos\varphi_0}{X_{SDT}C_{DC}}\ , GG_2=\frac{C_0\sin\varphi_0}{X_{SDT}C_{DC}} \quad (26)$$
$$FF_B=\ (1+\frac{X_L}{X_{SDT}})$$

The quantities of network, induction motor and STATCOM are specified before. Generally, the linearized state model for Equations 19 and 20 are expressed as:

$$X^0 = AX + BU \quad (27)$$

$$Y = CX \quad (28)$$

That

$$A=[A_{STATCOM}], B=[B_{STATCOM}]\ and\ C=\left[C_{STATCOM_\omega}\right] \quad (29)$$

Taking the Laplas transform of Equations 27 and 28 ,we get:

$$sX(s) = AX(s) + BU(s) \quad (30)$$

$$Y(s) = CX(s) = C(sI - A)^{-1}BU(s) \quad (31)$$

Therefore, the plant transfer function will be calculated as:

$$P = \frac{Y(s)}{U(s)} = C(sI - A)^{-1}B \quad (32)$$

5. Simulation Results

The algorithm flowchart of Figure 4 is considered to design the robust controller for the quoted system. The system parameters at nominal operating point are specified before. The nominal operating point for the design is computed for an infinite bus voltage of $1\ p.u$ at unity power factor (PF), so $V_{q\infty} = 1\ p.u$, $V_{dq\infty} = 0\ p.u$ and two important STATCOM parameters, $C = 1\ p.u$ and $V_{DC} = 1\ p.u$.

5.1 GLS Method

The nominal plant transfer function for the selected operating point is computed as:

$$P_1 = \frac{p_4 s^4 + p_3 s^3 + p_2 s^2 + p_1 s + p_0}{q_6 s^6 + q_5 s^5 + q_4 s^4 + q_3 s^3 + q_2 s^2 + q_1 s + q_0} \quad (33)$$

Where

$$\begin{gathered} p_4 = 1201;\ p_3 = -2.515 * 10^5;\ p_2 = -7.968 * 10^6; \\ p_1 = -5.265 * 10^7;\ p_0 = -4.683 * 10^5; \\ q_6 = 1;\ q_5 = 85.82;\ q_4 = 1.701 * 10^5; \\ q_3 = 5.831 * 10^6 \\ q_2 = 3.625 * 10^8;\ q_1 = 5.864 * 10^9;\ q_0 = 5.683 * 10^6 \end{gathered} \quad (34)$$

Off nominal infinite bus voltage between the ranges of 1-0.1 $p.u$ and power factor between the ranges of 1-0 lagging which give steady state stable situation, are considered in the robust design. The dB magnitude versus frequency plots for the nominal plant $P(j\omega)$ and perturbed plant $\tilde{P}(j\omega)$ should be determined. The quantity $\left|\frac{\tilde{P}(j\omega)}{P(j\omega)} - 1\right|$ for each perturbed plant is constructed and the upper envelope in the frequency plane is fitted to the following function:

$$W_2 = \frac{0.2\, s^2 + 8.4\, s + 7.2}{1.1\, s^2 + 8.9 s + 24.9} \quad (35)$$

So $(\left|\frac{\tilde{P}(j\omega)}{P(j\omega)} - 1\right| \leq W_2(j\omega)$. A butterwort filter, which satisfies the properties of $W_1(s)$ is selected as [18]:

$$W_1 = \frac{K_d {f_c}^2}{s^3 + 2s^2 f_c + 2s{f_c}^2 + {f_c}^3} \quad (36)$$

Values of K_d =0.01 and f_c=0.5 are observed to be fulfill the requirements on the open loop transfer function L that is specified in Equations 17 and 18. For W_1 and W_2 selected above and for choice of the open loop transfer function L as:

$$L = \frac{0.62(s+500)(s+4)^2(s+0.012)}{(s+16.95)(s+0.05)(s+0.015)(s^2+4.23s+14.4)} \quad (37)$$

The controller transfer function obtained through the relation $C = \frac{L}{P_1}$ is:

$$C = \frac{p_5 s^5 + p_4 s^4 + p_3 s^3 + p_2 s^2 + p_1 s + p_0}{q_5 s^5 + q_4 s^4 + q_3 s^3 + q_2 s^2 + q_1 s + q_0} \quad (38)$$

$$\begin{gathered} p_5 = -4.363 * 10^{13};\ p_4 = -2.474 * 10^{16}; \\ p_3 = -8.83 * 10^{18};\ p_2 = -3.8 * 10^{21}; \\ p_1 = -7.173 * 10^{22};\ p_0 = -6.818 * 10^{24}; \\ q_5 = 1;\ q_4 = -8.448 * 10^{16};\ q_3 = 1.786 * 10^{19}; \\ q_2 = 5.237 * 10^{20};\ q_1 = 3.343 * 10^{21}; \\ q_0 = 1.663 * 10^{20} \end{gathered} \quad (39)$$

The plots for the nominal and robust performance criteria are shown in Figure 5. It can be observed that the nominal performance measure ($W_1 S$) is very small relative to 0 dB and well satisfied. The combined robust stability and performance measure ($W_1 S + W_2 T$) has a small peak at the corner frequency that is related to parameters of system considered in design and comparable to [20].

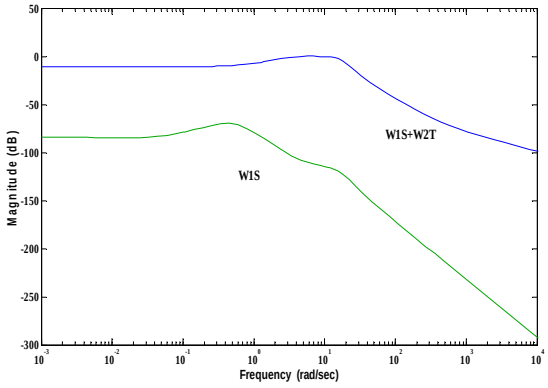

Figure 5: The robust and nominal performance with consideration to step response of motor's rotor speed

Once the robust stability and performance criteria are plotted in Figure 5 are met, the stability and performance of the closed loop system have to be checked by direct simulation of the system dynamic equations. Figure 6 shows the step response of motor's rotor speed (ω_{rm}) during starting with controller at mentioned nominal operating point.

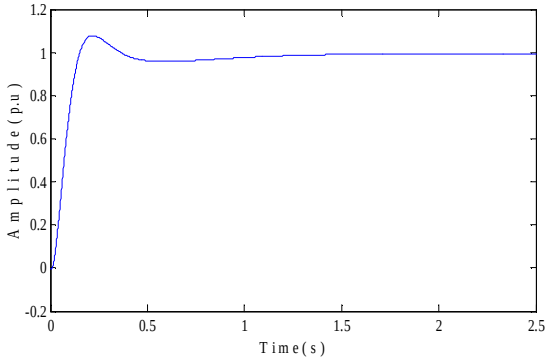

Figure 6: Step response of motor's rotor speed with GLS method

Fine Tuning on the controller parameters are performed from monitoring of the transient response of the system. The distortion of the speed response is very small with

peak value 8% and has a satisfactory dynamic performance. The effectiveness of the robust design is tested for a number of other operating conditions. Changing of operating points due to system parameters is considered as a changing of system voltage. Figure 7 shows the step response of motor's rotor speed for the following four operating status:
Infinite bus voltage=1 $p.u$, power factor=1; Infinite bus voltage=1 $p.u$, power factor=0.9
Infinite bus voltage= 0.9 $p.u$, power factor=0.9; Infinite bus voltage=0.9 $p.u$, power factor=0.7

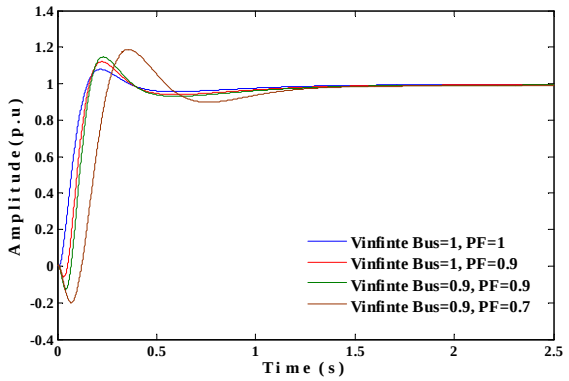

Figure 7: Effectiveness of changing of operating point due to system voltage on step response of motor's rotor speed (GLS method)

Whereas, V_{DC} and C are important factors in designing of STATCOM, therefore variation of these parameters are also considered in the robustness assessment of the designed controller. Figure 8 displays the step response of motor's rotor speed for the subsequent four operating conditions:
C=1, V_{DC}=1; C=0.9, V_{DC}=0.7;
C=0.6, V_{DC}=0.4; C=0.4, V_{DC}=0.35;

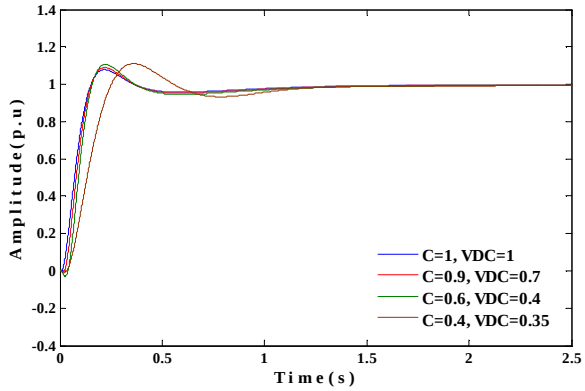

Figure 8: Effectiveness of changing of operating point due to STATCOM parameters on step response of motor's rotor speed (GLS method)

It can be realized that the suggested controller is very effective in providing damping for such varying operating circumstances. Tables 1 and 2 display and compare different specifications of the step response for the mentioned operating points.

Expectedly the influence of the controller will reduce as the operating point moves further and further away from the nominal value. It should be considered that the effectiveness of changing of operating point due to system voltage is more serious than changing of operating point due to STATCOM parameters of, so the settling time in Table 1 with 10% variation of $V_{Infinite\ Bus}$ and 30% variation of PF, reaches from 0.28 *sec* to 1.07 *sec* , but in Table 2 with 60% differentiation of C and 65% differentiation of V_{DC},

Table 1: Specifications of step response of motor's rotor speed with different system voltage (GLS method)

Description of System	Peak Time (sec)	Peak Value (p.u)	Rise Time (sec)	Settling Time (sec)
$V_{Infinite\ Bus} = 1, PF = 1$	0.21	1.08	0.10	0.28
$V_{Infinite\ Bus} = 1, PF = 0.9$	0.23	1.12	0.08	0.78
$V_{Infinite\ Bus} = 0.9, PF = 0.9$	0.24	1.14	0.07	0.87
$V_{Infinite\ Bus} = 0.9,$ $PF = 0.7$	0.35	1.19	0.11	1.07

settling time is obtained 0.96 *sec.* Besides, the peak value in Table 1 and Table 2 varies from1.08 $p.u$ to 1.19 and 1.12 $p.u$ respectively, that variation of settling time and peak value in Table 2 with different STATCOM parameters are lower than Table 1 values with different system voltage. It can be concluded from Figures 7 and 8 that there is maximum 18.98% under shoot when system voltage changes, so this quantity when STATCOM parameter varies, is little (0.54 %).

Table 2: Specifications of step response of motor's rotor STATCOM parameters (GLS method)

Description of System	Peak Time (sec)	Peak Value (p.u)	Rise Time (sec)	Settling Time (sec)
$C = 1, V_{DC} = 1$	0.21	1.08	0.10	0.28
$C = 0.9, V_{DC} = 0.7$	0.22	1.09	0.09	0.29
$C = 0.6, V_{DC} = 0.4$	0.23	1.10	0.08	0.72
$C = 0.4, V_{DC} = 0.35$	0.36	1.12	0.15	0.96

5.2 PI Controller

Figure 9 shows the step response of motor's rotor speed with GLS method that has been obtained before and compares it with PI controller. It is obviously indicated that GLS method has better dynamic attitude than PI controller so the conventional controller has high fluctuations to reach the steady state position. The comparison between the specifications of GLS method and PI controller proves that quantity of overshoot in PI controller is higher than GLS method, also the amount of undershoot in GLS method is obviously lower than PI controller. Although the peak time in PI controller is lower than GLS method. The PI controller designed is checked for the number of other operating points that has been defined before when the step response of

motor's rotor speed of was considered. Figures 10 and 11 display the step response of motor's rotor speed for these operating conditions.

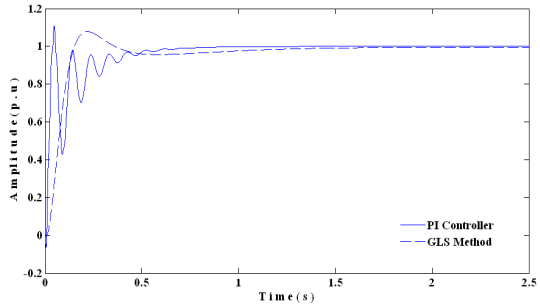

Figure 9: Comparison between the step Response of motor's rotor speed with PI controller and GLS method

It can be observed that this method is not very strong against changing of system voltage and STATCOM parameters when compare with GLS method that responses have been shown in Figures 7and 8, even the system goes to instability with 10% variation of $V_{Infinite\ Bus}$ and 30% variation of PF. Also, it should be considered that the effectiveness of changing of operating point due to system voltage is more acute than changing of STATCOM parameters, similar to GLS method.

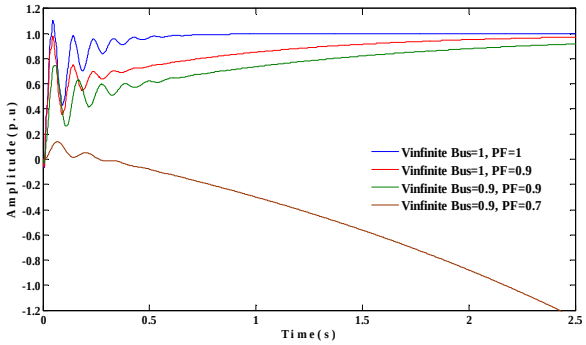

Figure 10: Effectiveness of changing of operating point due to system voltage on step response of motor's rotor speed with PI controller

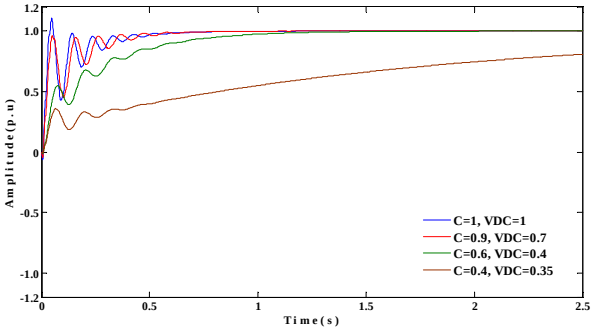

Figure 11: Effectiveness of changing of operating point due to STATCOM parameters on step response of motor's rotor speed with PI controller

6. Conclusion

In this paper, a method of designing H_∞ robust loop shaping damping controller for a STATCOM in a power system consist of a large induction motor with STATCOM installed on its terminal, a transmission line and infinite bus through control of motor's rotor speed is proposed. The design is performed utilizing both robust stability and robust performance considerations and a robust control design for STATCOM is proposed using H_∞ control by means of GLS method. The design employed a nominal operating point at $V_{Infinite\ Bus} = 1\ p.u$ and the perturbations in the range of $V_{Infinite\ Bus} = 1\text{-}0.9\ p.u$ and $PF = 1\text{-}0.7$for changing of operating point due to system voltage and C=1-0.4 and V_{DC} =1-0.35 $p.u$ for changing of operating point due to STATCOM parameters. Step response of motor's rotor speed with robust loop shaping control has been found to be very effective in the mentioned range of operating conditions. The robust controllers is compared with a conventional PI controller and this is definitely shown that this method is not very strong against changing of system voltage and STATCOM parameters when compare with GLS method, even with $V_{Infinite\ Bus} = 0.9\ p.u$ and PF =0.7, the system goes to instability. It is clearly indicated that GLS method has better dynamic behavior than PI controller so the conventional controller has high oscillations to reach the steady state position. It is shown that quantity of overshoot in PI controller is higher than GLS method, also the amount of undershoot in GLS method is apparently lower than PI controller, although the peak time in PI controller is lower than GLS method.

7. References

1. Khuntia, S.R., et al., *A Comparative Study of PI, IP, Fuzzy and Neuro-Fuzzy Controllers for Speed Control of DC Motor Drive*. International Journal of Electrical Systems Science and Engineering, 2009. 1(1).

2. Wu, Q. and C. Shao. *Novel hybrid sliding-mode controller for direct torque control induction motor drives*. in *American Control Conference*. 2006. Minnesota, USA: IEEE.

3. Gomez, J.C., et al., *Behavior of induction motor due to voltage sags and short interruptions.* Power Delivery, IEEE Transactions on, 2002. 17(2): p. 434-440.

4. Hedayati, M., et al., *Investigating the Performance of Shunt FACTS for the Operation of Induction Motors under Different Voltage Sag Conditions.* Journal of Applid Sciences, 2010. 10: p. 3014-3020.

5. Huweg, A.F., S.M. Bashi, and N. Mariun. *A STATCOM simulation model to improve voltage sag due to starting of high power induction motor*. in *Power and Energy Conference, 2004. PECon 2004. Proceedings. National*. 2004.

6. Javanbakht, P. and M. Abedi, *The Enhancement of Dynamic Performance of Cascaded Induction Motors Using SVC and D-STATCOM.* International Journal of Electrical and Power Engineering, 2008. 2(6): p. 415-424.

7. Hedayati, M. and H. Oraee. *Assessment Study Of Shunt FACTS Devices For Improving Dynamic Behavior Of Induction Motors*. in *Power Electronics and Drives Systems, 2005. PEDS 2005. International Conference on*. 2005.

8. Tadeo, F., O.P. Lopez, and T. Alvarez, *Control of neutralization processes by robust loop shaping.* Control Systems Technology, IEEE Transactions on, 2000. 8(2): p. 236-246.

9. Farsangi, M.M., et al., *Robust FACTS control design using the H∞ loop-shaping method.* Generation, Transmission and Distribution, IEE Proceedings-, 2002. 149(3): p. 352-358.

10. Zhou, K., J.C. Doyle, and K. Glover, *Robust and optimal control*. 1996: Prentice-Hall Englewood Cliffs, NJ.

11. Chuanjiang, Z., et al., *Robust power system stabilizer design using H Infinite loop shaping approach.* Power Systems, IEEE Transactions on, 2003. 18(2): p. 810-818.

12. Majumder, R., et al., *LMI approach to normalised H Infinite loop-shaping design of power system damping controllers.* Generation, Transmission and Distribution, IEE Proceedings-, 2005. 152(6): p. 952-960.

13. Lin, J.L. and L.G. Shiau, *On stability and performance of induction motor speed drives with sliding mode current control.* Asian Journal of Control, 2000. 2(2): p. 122-131.

14. Katayama, S., K. Yubai, and J. Hirai, *Iterative Design of the Reduced-Order Weight and Controller for the H Infinite Loop-Shaping Method Under Open-Loop Magnitude Constraints for SISO Systems.* Industrial Electronics, IEEE Transactions on, 2009. 56(10): p. 3854-3863.

15. Majumder, R., et al., *Design and real-time implementation of robust FACTS controller for damping inter-area oscillation.* Power Systems, IEEE Transactions on, 2006. 21(2): p. 809-816.

16. McFarlane, D. and K. Glover, *A loop-shaping design procedure using H Infinite synthesis.* Automatic Control, IEEE Transactions on, 1992. 37(6): p. 759-769.

17. Rahim, A.H.M.A., S.A. Al-Baiyat, and H.M. Al-Maghrabi, *Robust damping controller design for a static compensator*. Generation, Transmission and Distribution, IEE Proceedings-, 2002. 149(4): p. 491-496.

18. Rahim, A. and E.P. Nowicki, *A robust damping controller for SMES using loop-shaping technique.* International Journal of Electrical Power & Energy Systems, 2005. 27(5-6): p. 465-471.

19. Shen, D. and J.B. Cruz. *An improved game theory based approach to one type of H-infinity optimal control problems*. in *American Control Conference, 2006*. 2006.

20. Rahim, A. and M.F. Kandlawala, *Robust STATCOM voltage controller design using loop-shaping technique.* Electric Power Systems Research, 2004. 68(1): p. 61-74.

21. Rahim, A. and E.P. Nowicki, *Performance of a grid-connected wind generation system with a robust susceptance controller.* Electric Power Systems Research, 2011. 81(1): p. 149-157.

22. Franz, S.H. and M.S. Triantafyllou, *System Design for Uncertainty*, in *http://ocw.mit.edu/courses/mechanical-engineering/2-017j-design-of-electromechanical-robotic-systems-fall-2009/course-text/MIT2_017JF09_coursetext.pdf*, 2009.